13th World Conference on Earthquake Engineering
Vancouver, B.C., Canada
August 1-6, 2004
Paper No. 2188

SEISMIC RISK ANALYSIS FOR CITY GAS NETWORK IN SOUTHERN KANTO AREA, JAPAN

Wataru NAKAYAMA[1], Yoshihisa SHIMIZU[2], Fumio YAMAZAKI[3], Junya FUKUOKA[4], Ryoji ISOYAMA[5], and Eisuke ISHIDA[6]

SUMMARY

We constructed a detailed seismic hazard model which shows possibility of ground motion during specific length of time, on every 50m square mesh based on recent knowledge of seismology. The superposition of seismic hazard data and damage estimation system on the GIS map makes it possible to calculate seismic risk of large-scale networks such as city gas supply networks. This paper introduces the recent development of GIS-based seismic hazard assessment to evaluate seismic risks for city gas networks, and the examples of its application are demonstrated. The result shows that 1) preventive measure for low pressure which have enormous length should be avoided because they constitute overspending. 2) In contrast, emergency response measure for the low-pressure networks is cost-effective.

INTRODUCTION

Several measures to reduce seismic risks had been planned and executed by most companies which are concerned about risk management. However, the effect of these measures cannot be easily estimated by companies which have large-scale networks. The reason for the difficulty is that there has not been any procedure to quantify seismic risks for complicated networks. Consequently, there has not been an answer to the question “How much risk has been removed by the measure?” or “Which measure for same purpose is more effective?” Although some researchers have studied earthquake risk analysis since the 1980's, a large-scale city gas network has not been a subject of such research.

Recently, Tokyo Gas Co. constructed a geographic information system (GIS), which contains data from 60,000 bore holes. It also developed a new disaster mitigation system “SUPREME” (Shimizu et al., 2002) [1] which includes a damage assessment system capable of calculating damage to low-pressure gas

[1] Assistant manager, Tokyo Gas Co. Ltd.., Tokyo, Japan. Email: wataru@tokyo-gas.co.jp
[2] Director, Tokyo Gas Co. Ltd.., Tokyo, Japan. Email: yshimizu@tokyo-gas.co.jp
[3] Professor, Chiba University, Chiba, Japan. Email: yamazaki@tu.chiba-u.ac.jp
[4] Assistant manager, Japan Engineering Consultants, Tokyo, Japan, Email: fukuokajy@jecc.co.jp
[5] Director, Japan Engineering Consultants, Tokyo, Japan, Email: Isoyama@jecc.co.jp
[6] Manager, Japan Engineering Consultants, Tokyo, Japan, Email: isidae@jecc.co.jp

pipelines in every 50m square mesh. Superposition of Seismic hazard data on GIS map makes it possible to calculate seismic risk of large-scale networks such as city gas supply networks. This paper introduces the recent development of GIS-based seismic hazard assessment to evaluate seismic risk for city gas networks, and examples of its application, by Tokyo Gas Company.

BASIC FLOWCHART OF RISK ANALYSIS

Fig. 1 shows flowcharts which explain how the process of seismic risk analysis is applied for prioritization for seismic retrofit. Seismic risk is estimated by direct and indirect expected loss of total gas supply system, that is,

$$TL_j = \Sigma_i (DL_j(i) + IL_j(i)) * P_j(i)_j \,. \qquad (1)$$

Here, $TL_{j\ :}$: expected loss at j-th point, $DL_j(i)$, $IL_j(i)$:direct and indirect loss at j-th point due to ground motion with the intensity of i, $P_j(i)$: probability of a specific seismic ground motion on the ground surface at the j-th point caused by i-th earthquake. Direct loss consists of repair cost, work expense for resumption of gas supply, and the decrease of an income by supply stop / supply reduction. Indirect damage may be exemplified by secondary damage due to the outbreak of fire, the spread of a fire, etc. resulting from the damage to pipes.

In this study, seismic hazard is evaluated and applied to complicated city gas networks, and cost effectiveness of several disaster prevention measures are estimated. This paper profiles a case of performance for rational earthquake measure investment through prioritization using estimated cost effectiveness.

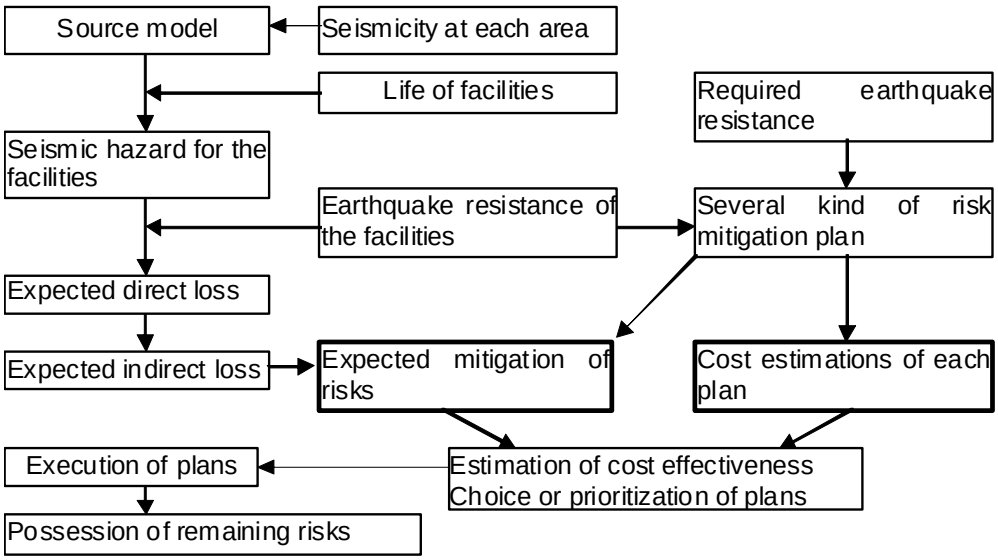

Fig. 1: Flow chart of the seismic risk assessment

BASIC FLOWCHART OF HAZARD ANALYSIS

Total process of hazard analysis is shown in Fig. 2.

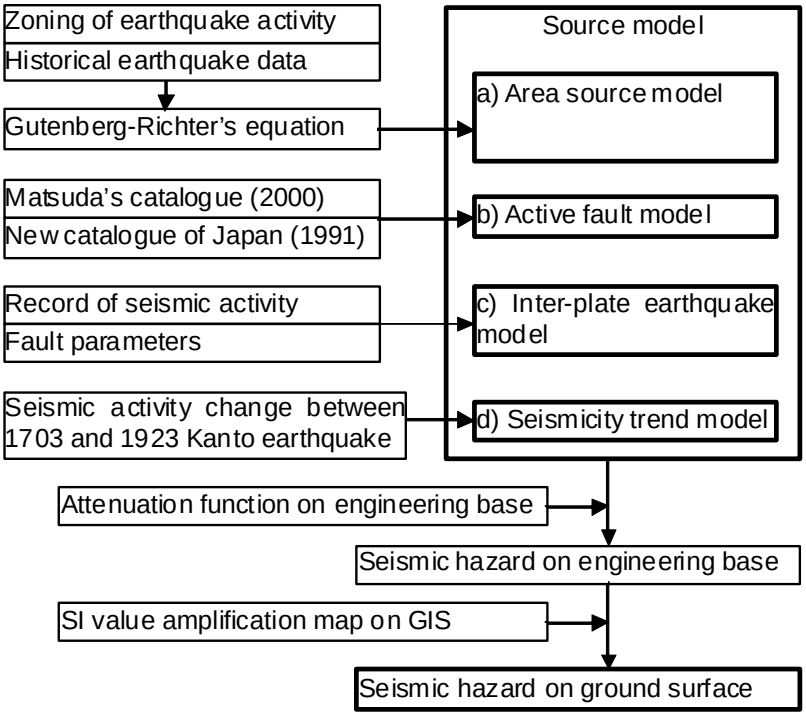

Fig. 2: Flow chart of the seismic hazard analysis

Four types of source model are constructed to calculate seismic hazard: a) area source using Gutenberg-Richter's equation calculated from historical earthquake database; b) active fault model taking into account change in probability, which depends on the time lapse since the latest activity and average interval of the occurrence of earthquake on each fault; c) inter-plate earthquake model for major recurrent earthquakes; and d) seismicity trend model for special features of activity change before major earthquakes in the Southern Kanto area.

As an index of ground motion strength for hazard models, it was decided to employ the SI value, which is generally used as the criterion for city gas supply suspension or damage presumption. Seismic hazard evaluation by each source model was performed using the attenuation function for SI value, which is thought to have a high correlation with damage on the engineering base of Vs=600 (m/s). Next, total seismic hazard on the engineering base was compounded on the assumption that seismic activity of each source does not have mutual interaction, in other words, they are statistically summed up independently. Finally, a fine (50m mesh square) seismic hazard map and hazard curve on the ground surface are constructed using an amplification map (50m mesh square) made by processing data from 60,000 boreholes [2]. Seismic risk assessment was done using the calculated seismic hazard values. The most suitable seismic retrofit program or development of a new emergency response system are chosen to reduce estimated seismic risks.

BASIC IDEA OF SEISMIC HAZARD DEFINED BY "PROBABILITY OF EXCEEDANCE (PE)"

For any given site on the map, the ground motion effect (e.g. SI value, peak ground acceleration) is calculated at the site for all the earthquake locations and magnitudes believed possible in the vicinity of the site. Each of these magnitude-location pairs is believed to happen at some average probability per year. Small ground motions are relatively likely; large ground motions are very unlikely.

Beginning with the largest ground motions and proceeding to smaller ones, we add up probabilities until we arrive at a total probability corresponding to a given probability, P, in a particular period of time, T. The probability P comes from ground motions larger than the ground motion at which we stopped adding. The corresponding ground motion is said to have a P probability of exceedance (PE) in T years. Once many pairs of PE and ground motion are calculated, seismic risks of any facilities are calculated based on PE at the same site. In this study, magnitude-location pairs on different sites are categorized as four types of source model to calculate PE.

CONSTRUCTION OF SOURCE MODEL

Historical seismicity model

We construct an area source model based on historical seismicity data (JMA magnitude +5.0 and depth -100km earthquakes) from JMA monthly reports (1926 – July 1996) that contain enough data for the construction. Since source parameters are unreliable and uncertain, we excluded pre-instrumental seismicity data before 1926, which were constructed on the basis of seismic damage reports. Distribution of instrumental earthquakes in and near Japan recorded by JMA is shown in Fig.3.

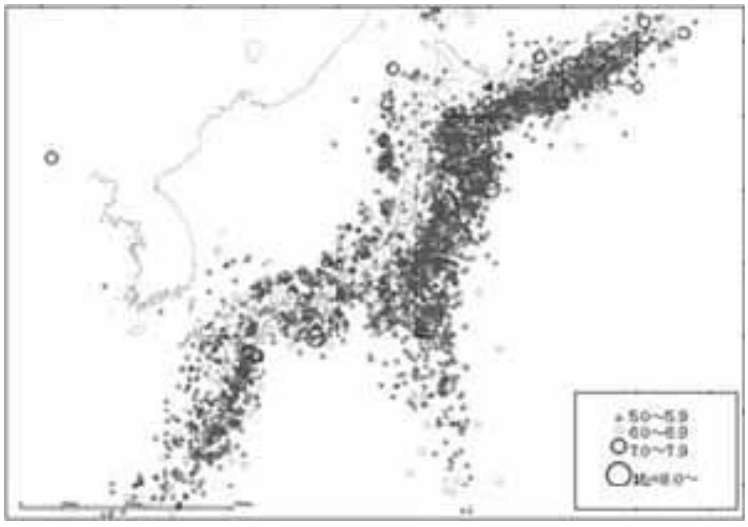

Fig. 3: Distribution of instrumental earthquakes (1926-1996)

Area source models for the Philippine Sea, Pacific, and 'Continental' (Eurasia and North-America) plates are partitioned in accordance with Annaka et al. (2001) [3]. In consideration of the subduction direction and the depth, the model for the Philippine Sea (Fig. 4), Pacific (Fig.5), and Continental plates (Fig.6) was prepared in three dimensions. These area source models projected on historical seismicity data, rates and magnitudes are summarized as Gutenberg-Richter equations,

$$\log(N_i[M > m] = a_i - b_i m\,, \qquad (2)$$

for each partition of area source. Here, *Ni*: cumulative number of earthquakes whose magnitude (*M*) is greater than *m* in *i*-th area. The values *ai* and *bi* are determined by the least square fit to the observed data.

We assume that an occurrence of earthquakes on this model is a random (Poisson) process in time described as,

$$p(\tau) = 1 - \exp(\nu_0 \tau). \quad (3)$$

Here, $p(\tau)$: probability of earthquake occurrence, τ: calculation period, ν_0: average annual number of earthquakes.

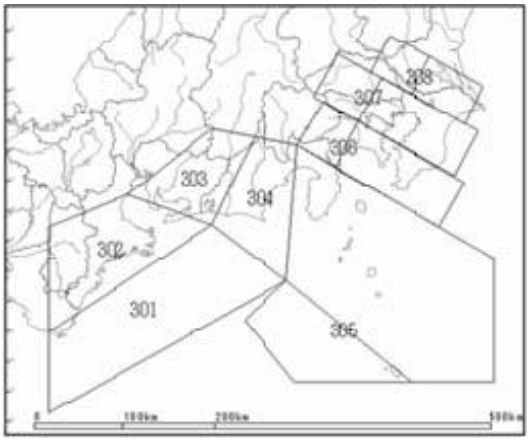

Fig. 4: Area source model for the Philippine Sea Plate

Fig. 5: Area source model for the Pacific Plate

Fig. 6: Area source model for the North America Plate and Eurasia Plate

Active fault model

To estimate seismic hazard, we employed the maximum magnitude model based on characteristic earthquake model (Schwarz and Coppersmith, 1984) [4], which proposes that the earthquake of maximum magnitude occurs repeatedly at almost the same interval. When the latest activity is unknown, the rate of earthquake occurrence is calculated using Poisson process. If the latest activity can be predicted from the geological dating of the previous event, we assume the log normal distribution, where probability of earthquake occurrence increases after the last previous event. We assumed 0.23 for the standard deviation of the log normal distribution according to the report by Headquarters for Earthquake Research Promotion (1999) [5]. The rate of earthquake occurrence for time-dependent source is estimated for 100 years starting from 2001. The configurations and locations of active faults are modeled based on "Active Fault in Japan –Sheet Maps and Inventories" [6], and fault parameters are based on the latest information in addition to that of Matsuda et al. (2000) [7]. The distribution of active faults used in this study is shown in Fig.7, and fault parameters for them are presented in Table 1.

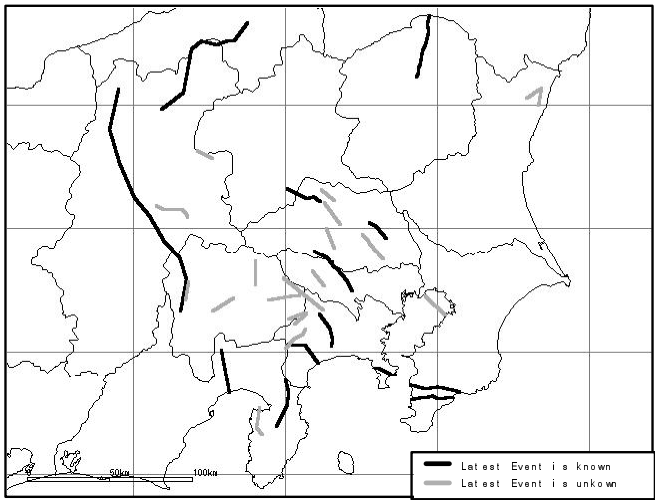

Fig. 7: Distribution of active faults in the Kanto Region

Table 1: Parameters of active faults in the Kanto Region

Active fault	Length (km)	Magnitude	Activity	Average slip rate (m/ky)	Recurrence interval (ky)	Elapsed time since latest event (ky)
Sekiya	40	7.5	A	5.00	0.6	0.3
North Kamogawa	29	7.3	AB	1.00	2.3	10.0
South Kamogawa	26	7.2	AB	1.00	2.1	6.0
Hirai-Kushibiki	20	7.0	B	0.25	7.9	10.0
Motoarakawa	16	6.8	B	0.30	6.9	5.0
Arakawa	20	7.0	B	0.20	8.0	-
Tachikawa	25	7.1	B	0.50	5.0	1.4
Kitatake	15.2	6.8	A	0.40	1.0	1.4
Isehara	13	7.0	B	0.50	3.3	1.1
Kannawa-Kohdu Matsuda	25	8.0	A	3.00	3.0	3.0
Tanna	30	7.3	A	2.00	1.2	0.07
Fujigawa Kakou	20	8.0	A	7.00	1.1	2.1
Shinanogawa	106	8.0	A	5.00	1.0	0.15
Itigawa-Shizuoka Chubu	100	8.0	A	14.00	1.0	1.2
Kirigamine	20	7.0	A	5.00	0.3	-
Asama Nishi	10	6.5	AB	1	0.8	-
Fukaya	10	6.5	B	0.3	2.6	-
Konan Imaichi-Sugaya	16	6.8	C	0.1	12.7	-
Ogose	13	6.7	C	0.05	20.7	-
Tsurukawa	30	7.3	C	0.05	47.7	-
Ougiyama	18	6.9	BC	0.1	14.3	-
Choujagoya	10	6.5	B	0.5	1.6	-
Doushigawa	10	6.5	BC	0.1	7.9	-
Kurokura	10	6.5	B	0.5	1.6	-
Daibosatsu-Touge Nishi	14	6.7	C	0.05	22.2	-
Sone-Kyuryou	15	6.8	B	0.5	2.4	-
Darumagawa	12	6.6	B	0.5	1.9	-
Sekiguchi-Kuroiso	10	6.5	D	0.005	158.9	-
Sekiguchi-Yonehira	10	6.5	D	0.005	158.9	-
Tokyowan Hokubu	25	7.2	B	0.1	19.9	-
Itsukaichi	10	6.5	C	0.05	15.9	-
Oonajika	10	6.5	B	0.5	1.6	-

Inter-plate earthquake model

Four (Kanto, Kanagawa-ken Seibu, Toukai and Tounankai) earthquakes are chosen to make an interplate earthquake model. Probability of earthquake occurrence is calculated in the same way as in the active fault model, based on information about latest activity. The magnitude is assumed to follow the maximum magnitude model. The Kanto Earthquake, which is recognized as the largest earthquake to occur in the Kanto area, is of two types: the greater Genroku Kanto (1703) type and the smaller Taisho Kanto (1923) type. The seismic source of the Genroku Kanto type is off Chiba in addition to a fault below Tokyo Bay, which slipped during the Taisho Kanto earthquake. In this study, these two faults are assumed to slip independently. The locations and fault parameters are based on "Fault Parameter Handbook" (1989) [8]. The source models for interplate earthquakes are shown in Fig. 8, and fault parameters, in Table2.

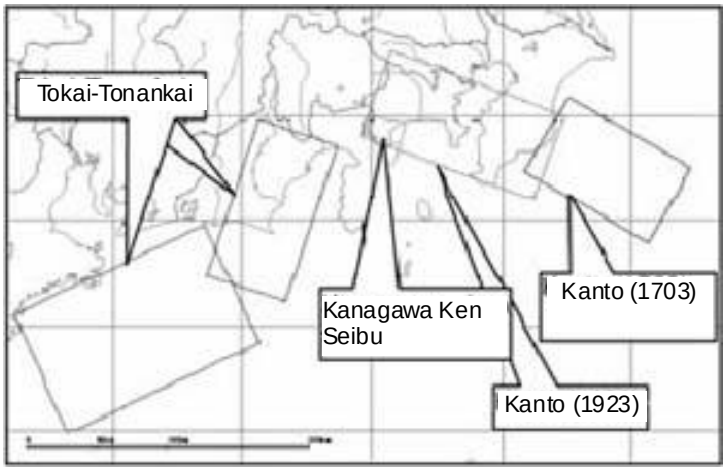

Fig. 8: Distribution of the source models for interplate earthquakes

Table 2: Parameters for interplate earthquakes

Earthquake	Magnitude (Mj)	Latest event(Yrs.)	Interval of events (Yrs.)
Kanto (1703) (Off Chiba fault)	7.9	1703	440
Kanto (1923)	7.9	1923	220
Tokai-Tonankai	8.1	1944	119
Kanagawa Ken Seibu	7.0	1923	73

Seismic model for increasing probability between major Kanto earthquakes

Seismic activity along the Sagami Trough below the Kanto Region is time-dependent, and increases from the last large interplate earthquake (Kanto Earthquake) to the next one. Usually, the activity in that region stops soon after the previous large earthquake, except for aftershocks. Since the area source model based on historical seismicity (1926-1996) mentioned above was constructed based on data from the dormant term, the model will underestimate the seismic hazard without any correction.

In this study, the data of seismic activity increase were extracted from a pre-instrumental earthquake catalogue which records major earthquakes that occurred during the 220 years between the Genroku Kanto Earthquake (1703) and the Taisho Kanto Earthquake. Earthquakes were extracted selecting only large earthquake with an SI value larger than 20 cm/sec in a circle with a radius [centering on the Tokyo Gas' head office] of 40km. Attenuation function is applied to this extraction process. The cumulative number of earthquakes selected is plotted in Fig.9. Twenty earthquakes have occurred during the 220 years between two Kanto earthquakes. It is particularly notable that occurrence was concentrated just

before the Taisho Kanto Earthquake. Only two earthquakes remained when the aftershocks of 1923 Kanto Earthquake were excluded. This change of seismic activity between large inter-plate earthquakes is quantitatively modeled and used for the analysis to evaluate future increase of seismic risk in Kanto area. In the above modeling process, aftershocks were excluded by the procedure proposed by the Public Works Research Institute, Ministry of Construction (1983) [9]. To predict future increase in seismic risk, exponential shaped function is applied to the data which show the cumulative number of earthquakes, and the frequency of earthquakes is estimated, as follows.

$$\nu=(0.52\exp(0.0163(x+78))-2)/\ x \qquad (4)$$

x: Particular period of time to calculate seismic hazard

ν: Frequency of earthquakes in x years (earthquakes/year)

The magnitude is presumed to be Mj = 6.6 as calculated from the average of the seismic moment of the earthquakes shown in Fig. 9, using the magnitude-moment relationship (Kanamori, 1977) [10]. The location of seismic source was modeled for distribution at random in the rectangular area (Solid line in Fig. 10) assumed from the distribution of earthquake (Dots in Fig. 10). For example, the rate of earthquake occurrence in this area is estimated to be about 0.075 (occurrence per year) using Equation (4) applied in the calculation period of 100 years.

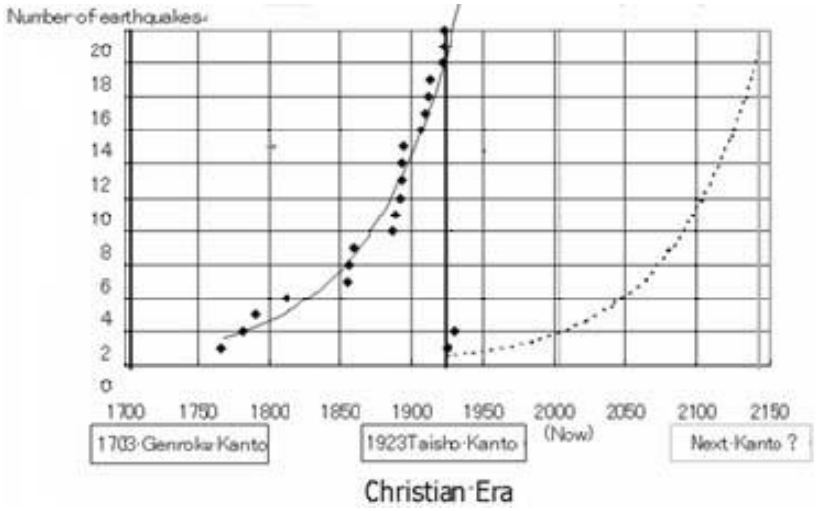

Fig. 9: Relationship between the Kanto Earthquake and the number of earthquakes in the Southern Kanto Region (SI>20kine)

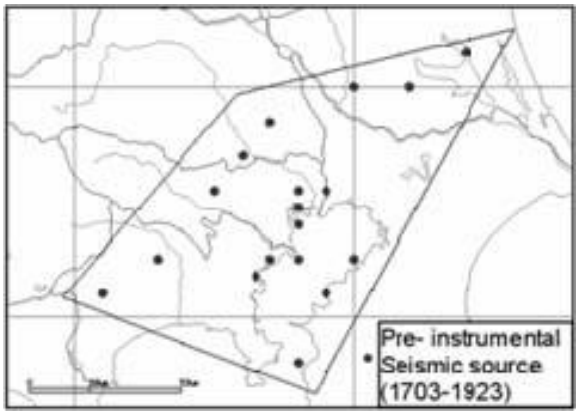

Fig.10: Area source model of the Southern Kanto Region considering time-dependent seismicity

SEISMIC HAZARD ON ENGINEERING BASE

The four seismic source models constructed are compounded independently from each other, and the total seismic hazard on the engineering base (Vs=600m/sec) is calculated. Seismic hazard in each source model is estimated using the attenuation function (Fig. 11) proposed by Shabestari and Yamazaki (1999) [11].
Fig.12 shows an example of a seismic hazard map obtained on the engineering base level (Vs=600m/s) for a 9.5% probability of exceedance in 100 years. This probability corresponds to ground motion with a recurrence period of 1,000 years. Higher seismic hazard is estimated to exist in the southern coastal area, area around the source of the Tokai (A) and Kanagawaken-Seibu (B) earthquakes, and the Itoigawa-Shizuoka tectonic line(C).

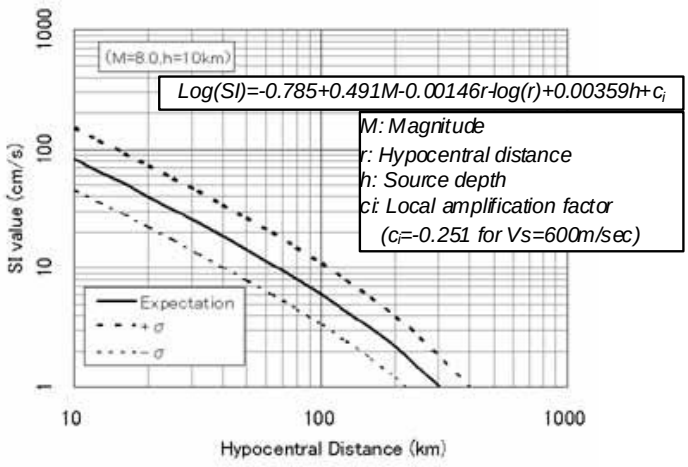

Fig.11: Attenuation function for the SI-value used in the analyses

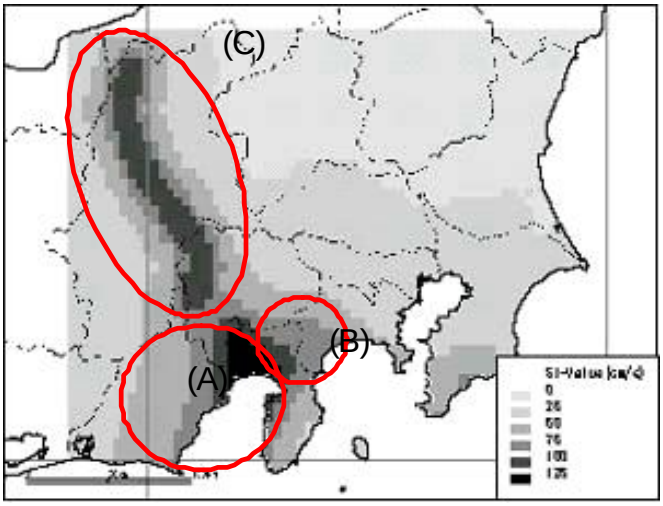

Fig.12: Seismic hazard map on the base rock level (Vs=600m/s)
(the probability of exceedance in 100 years: 9.5%)

Fig.13 shows the hazard (PE: probability of exceedance) curve estimated on the engineering base level below the head office of Tokyo Gas Co. In a 100-year period, a value of 30kine has a 14% probability of exceedance, and 60kine, one of 1.3%. At low ground motion, the effect of the historical earthquake model and the time-dependent model is larger than that of other models. At a ground motion greater than 30kine, the effect of the interplate earthquake model is dominant. The analysis did not find any significant effect with the active fault model. This result shows that there is no active fault whose next earthquake is expected to occur in near future in the Kanto Region.

SEISMIC HAZARD ON GROUND SURFACE

To take into account the characteristics of surface foundation, SI value amplification factors on GIS (Fig.14) estimated for every 50m mesh square using data from 60,000 bore holes are multiplied by the seismic hazard values obtained on the engineering base level for calculation of the seismic hazard at ground surface. SI value amplification is estimated to be high in the eastern part of the Tokyo Area (A) in Fig. 14.

Fig.15 shows the SI value distribution at ground surface for the 39.5% probability of exceedance in 100 years. This probability corresponds to ground motion with a recurrence period of 200 years. There is estimated to be a high seismic hazard in the eastern part of Tokyo (A), where SI amplification is large, in addition to the southern part (B) where a high seismic hazard is obtained on the engineering base level.

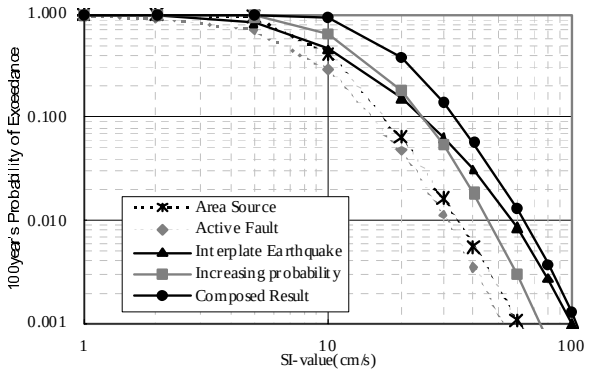

Fig.13: Seismic hazard curve on the base rock (Vs=600m/s)

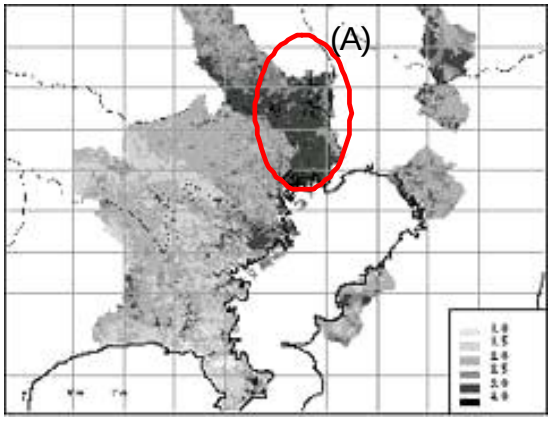

Fig.14: Distribution of the amplification ratio of SI-value

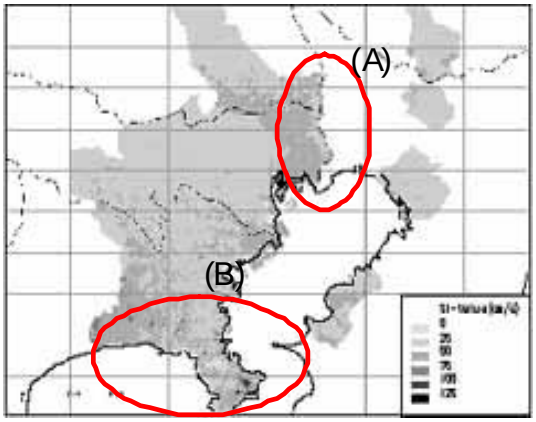

Fig.15: Seismic hazard map on the ground surface
(the probability of exceedance in 100 years: 39.5%)

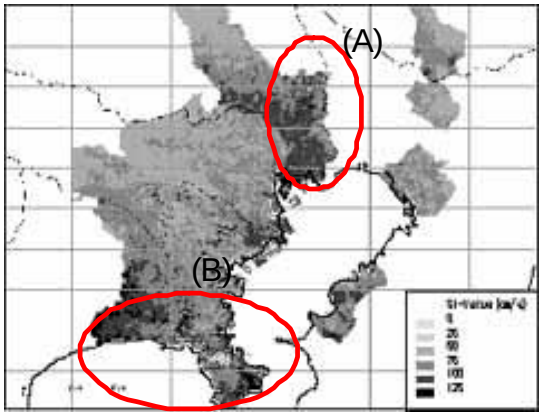

Fig.16: Seismic hazard map on the ground surface
(the probability of exceedance in 100 years: 9.5%)

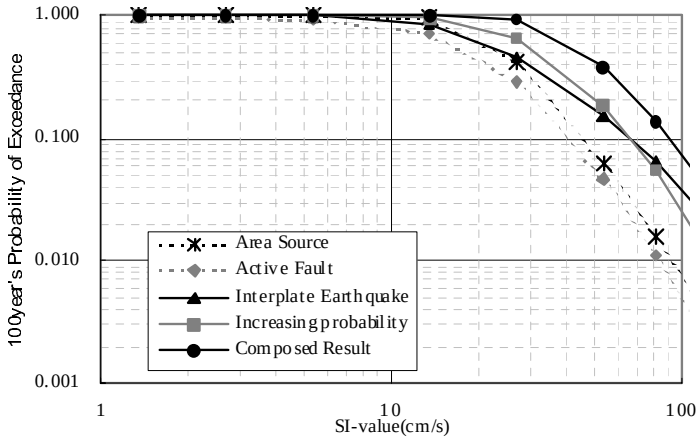

Fig.17: Seismic hazard curves on the ground surface

Fig.16 shows the SI value distribution at ground surface for the 9.5% probability of exceedance in 100 years (corresponding to Fig.12). In this map, the SI value is estimated to be larger than 60 kine in the whole supply area of Tokyo Gas Co. and 100 kine at area (A) and (B). From a different viewpoint, hazard (PE: probability of exceedance) may also be expressed as curves (Fig. 17) on the ground surface at the head office of Tokyo Gas Co. A value of 30 kine has 81% probability of exceedance, and 60 kine has 29%

PE in 100 years.

RISK ANALYSIS FOR LOW PRESSURE NETWORK

Estimation of damage probability to low-pressure pipes

Expected values of breaks for low-pressure pipes in a 100-year period are calculated by the damage estimation function of SUPREME (Shimizu et al., 2002) [1] based on estimated seismic hazard. The seismic hazard obtained is probability of exceedance (PE), so that the probability P corresponding to a specific SI value should be determined by differentiating PE with respect to the SI value. The projected number of pipe breaks (*NDLj*) at *j*-th point due to ground motion with the intensity of *SIi* is calculated using the following formula.

$$NDL_{ij} = P_j(SI_i) \times DL_j(SI_i). \qquad (5)$$

Here, *DLj(SIi)* is a fragility curve with respect to the SI value, based on the pipe damage experience in past earthquakes. The total damage probability of the network is obtained by adding *i* and *j*. Fig. 18 presents the projected number of pipe breaks in each section (block) of the gas supply network. The total number of projected pipe breaks in Tokyo Gas supply area was 1,050 for 15 years and 8,800 for 100 years. These results show pipe breaks comparable to those in the Great Hanshin Earthquake (Kobe) (5,190 breaks in distribution pipes) may be expected to occur in its supply area within the next 100 years.

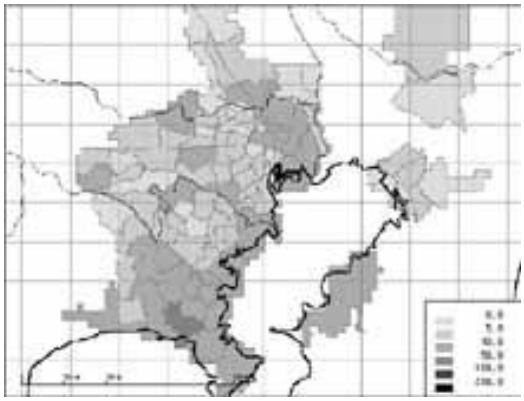

Fig.18: Expected value of breaks for low-pressure pipes in 15-year period

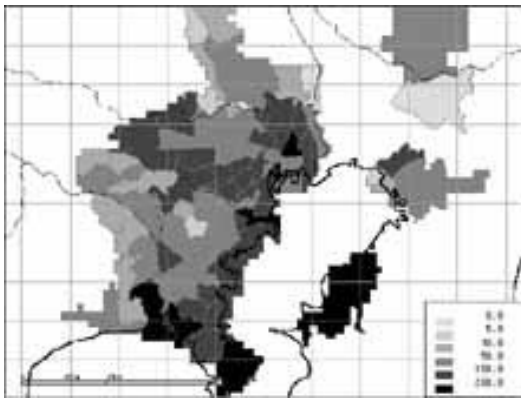

Fig.19: Expected value of breaks for low-pressure pipes in 100-year period

Choice of measure

In the Kobe Earthquake, numerous breaks in distribution and service pipes in low-pressure networks were reported, but little damage occurred to pipes with higher earthquake resistance. Thus, damage will be prevented all pipes with low earthquake resistance are replaced before the next large earthquake. However, such a preventive measure would require an enormous cost because the extended length of low-pressure pipes is more than 40,000km.

Another option is the new seismograph (new SI sensor) developed (Koganemaru et al, 2000) [12] to shut off district regulator (equipment which lowers gas pressure from medium to low) to stop supply of only low-pressure gas. SUPREME can be used as a real-time damage mitigation system which employs the new SI sensors with remote shut-off equipment installed at 3,700 district regulators in the Tokyo Gas supply area. Quick shut-off of gas supply by SUPREME will be able to prevent secondary disaster caused by numerous leaks from low-pressure pipes. Generally, this kind of emergency measure entails a much lower cost than the preventive measures mentioned above.

Estimation of cost effectiveness

Here, the cost effectiveness of two methods to prevent secondary disaster due to low-pressure gas is estimated and compared. While preventive measures such as replacement of low-pressure pipes have not been carried out by Tokyo Gas, the cost effectiveness is calculated for comparison with that of the emergency response measures already carried out (see Table 3).

Table 3: Cost effectiveness of measures for low-pressure network

The choice of measure	Type of measure	Cost effectiveness
Replacement of all low-pressure pipes	Preventive	< 100%
Installation of New SI sensors at 3700 district regulators	Emergency	> 100%
SUPREME system in addition to New SI sensors	Emergency	> 100%

It was confirmed that the preventive measure, which entails an enormous construction cost, is overly expensive and to be avoided. In contrast, the cost effectiveness of the emergency response measure is sufficient.

CONCLUSION

The new method of assessing seismic hazard for large-scale city gas networks enabled quantitative estimation of cost effectiveness of plan to prevent secondary disaster By checking cost effectiveness, companies can avoid overspending for earthquake disaster prevention. The major conclusions of this study are as follows,

1. New detailed (every 50m mesh square) seismic hazard assessment which consists of four source models; historical earthquakes, active fault earthquakes, inter-plate earthquakes, and time-dependent seismicity between great Kanto earthquakes.
2. The new seismic hazard assessment showed that the southern part of Kanagawa and eastern part of Tokyo have greater possibility of large ground motion than other areas.
3. Damage probability for complicated and vast amount of city gas network can be estimated by the new seismic hazard assessment.
4. Preventive measures for the low-pressure network should be avoided because they constitute overspending.
5. In contrast, emergency response measures for the low-pressure network are cost-effective

REFERENCES

1. Shimizu, Y., Yamazaki, F., Nakayama, W., Koganemaru, K., Ishida, E., and Isoyama, R., (2002): "Development of Super High-density Real-time Disaster Mitigation System for Gas Supply Networks", *12th European Conference on Earthquake Engineering*, Paper No.858, 10p.
2. Ishida, E., Isoyama, R., Yamazaki, F., Shimizu, Y. and Nakayama, W., (2001.8): "Preparation of Spatial Distribution of Site Amplification Factor of SI Value using GIS", *26th JSCE Earthquake Engineering Symposium*, Vol.1, pp.421-424.
3. Tadashi ANNAKA, Masayoshi SHIMADA, Tomohiko HIROSHIGE,(2001.8): "Model of estimating uncertainty for seismic hazard curves of around Kanto region based on Monte Carlo approach", Proceedings of the *26th JSCE Earthquake Engineering Symposium*, pp.133-136, (in Japanese)
4. Schwarz, D.P. and Coppersmith, K.J. (1984): "Fault behavior and characteristic earthquakes: Examples from the Wasatch and San Andreas fault zones.", *J. Geophys. Res.*, 89, 5681―5698.
5. Headquarters for Earthquake Research Promotion (1999): "Regarding the revised proposal 'About methods for evaluating long-term probability of earthquake occurrence'" (in Japanese).
6. The Research Group for Active Faults of Japan (ed.), (1991): "Active Fault in Japan-Sheet Maps and Inventories", *University of Tokyo Press* (in Japanese).
7. Tokihiko MATSUDA, Tomomi TSUKAZAKI and Mari HAGINOYA, (2000): "Distribution of active faults and historical shallow earthquakes of Japanese Islands, with a catalog of on-land seismogenic faults and earthquakes", *Active Fault Research*, No.19, pp.33-54 (in Japanese).
8. Ryosuke SATO (ed.), (1989): "Fault Parameter Handbook", *Kajima Institute Publishing*, (in Japanese)
9. Earthquake Disaster Prevention Department, Public Works Research Institute (PWRI), Ministry of Construction, (1983): "Investigations of the number and scale of foreshocks and aftershocks", *PWRI document*, Nos. 1995 (in Japanese).
10. Kanamori, H., (1977): "The energy release in great earthquakes", *J. Geophys. Res.*, 82, 2981-2987.
11. Shabestari, T.K., and F. Yamazaki, (1999): "Attenuation relation of strong ground motion indices using K-NET records", *25th JSCE Earthquake Engineering Symposium*, pp. 137-140.
12. Koganemaru, K., Shimizu Y., Nakayama W., Yanada T., Furukawa H., and Takubo K., (2000): "Development of a New SI Sensor", *12th World Conference on Earthquake Engineering*.